Article

Synthesis and Characterization of Catecholato Copper(II) Complexes with Sterically Hindered Neutral and Anionic N3 Type Ligands: Tris(3,5-diisopropyl-1-pyrazolyl)methane and Hydrotris(3,5-diisopropyl-1-pyrazolyl)borate

Kiyoshi Fujisawa [1,2,*], **Tetsuya Ono [2] and Moemi Okamura [1]**

[1] Department of Chemistry, Ibaraki University, Mito, Ibaraki 310-8512, Japan; 19nm008g@vc.ibaraki.ac.jp
[2] Department of Chemistry, Graduate School of Pure and Applied Sciences, University of Tsukuba, Tsukuba 305-8571, Japan; cu_peroxo@yahoo.co.jp
* Correspondence: kiyoshi.fujisawa.sci@vc.ibaraki.ac.jp; Tel.: +81-29-853-8373

check for updates

Abstract: Three catecholato copper(II) complexes, **[Cu(catCl$_4$)(L1′)]**, **[Cu(catBr$_4$)(L1′)]**, and **[Cu(catCl$_4$)(L1H)]**, supported by sterically hindered neutral and anionic N3 type ligands: tris(3,5-diisopropyl-1-pyrazolyl)methane (referred to as L1′) and hydrotris(3,5-diisopropyl-1-pyrazolyl)borate (referred to as L1$^-$), are synthesized and characterized in detail. Their X-ray structures reveal that both **[Cu(catCl$_4$)(L1′)]** and **[Cu(catBr$_4$)(L1′)]** complexes have a five-coordinate square-pyramidal geometry and **[Cu(catCl$_4$)(L1H)]** complex has a four-coordinate square-planar geometry. The L1H is unusual protonated ligand that controls its overall charge. For the three catecholato copper(II) complexes, the oxidation state of copper is divalent, and catechol exists in catecholate as two minus anion. This difference in coordination geometry affects their d-d and CT transitions energy and ESR parameters.

Keywords: copper complex; X-ray structure; catechol; non-innocent ligand; physicochemical property

1. Introduction

Transition metal complexes ligated by the hydrotris(pyrazolyl)borate as an anionic nitrogen-containing tripod ligand, as first prepared by Professor S. Trofimenko in 1966, are widely studied compounds [1]. An important advance in this chemistry is the introduction of alkyl substitutions of the pyrazolyl rings at the 3 (and 5) position(s) to prevent the formation of an inert hexa-coordinate compound [2]. The coordination behavior of transition metal complexes can easily be changed by introducing substituents with different electronic and steric properties on the pyrazolyl rings. Therefore, transition metal complexes based on these ligands have attracted a great deal of interest, and are still undergoing many investigations [3,4].

On the other hand, isoelectronic tris(pyrazolyl)methane ligands have received less attention. This ligand is formally derived from hydrotris(pyrazolyl)borate ligand, in which the central boron atom is replaced by a carbon atom. This tris(pyrazolyl)methane was also prepared by Professor S. Trofimenko in 1970 as a neutral nitrogen-containing tripod ligand [5]. Some researchers have improved the synthetic method of this ligand, including Elguero and co-workers [6], Reger and co-workers [7], and us [8,9]. We found that tris(pyrazolyl)methane could be synthesized in high yields using an autoclave [8,9].

By using these ligands of L$^-$ (hydrotris(pyrazolyl)borate) and L′ (tris(pyrazolyl)methane), structural differences in chlorido and nitrato copper(II) complexes were observed: neutral

four-coordinate [CuCl(L)] versus neutral five-coordinate [CuCl$_2$(L')] [8], neutral four-coordinate [CuCl(L)] versus cationic four-coordinate [CuCl(L')](ClO$_4$) [10], mononuclear [CuCl(L)] versus binuclear [Cu(μ-Cl)(L')]$_2$(ClO$_4$)$_2$ [11] and bidentate [Cu(κ^2-O$_2$NO)(L)] versus monodentate [Cu(κ-ONO$_2$)$_2$ (L')] [8,12], and their different electron donation properties in copper(I) carbonyl complexes: [Cu(CO)(L)] (ν(CO), 2056 cm^{-1}) versus [Cu(CO)(L')](PF$_6$) (ν(CO), 2107 cm^{-1}) [9].

In this research, we expanded our copper(II) coordination chemistry toward catecholato complex, since the interaction between copper and catechol has been reported in copper-containing proteins such as catechol oxidase and tyrosinase [13–16]. Moreover, catechol itself is known as "non-innocent" ligand [17–24] and is a redox active ligand that reversibly undergoes one-electron sequences illustrated in Scheme 1.
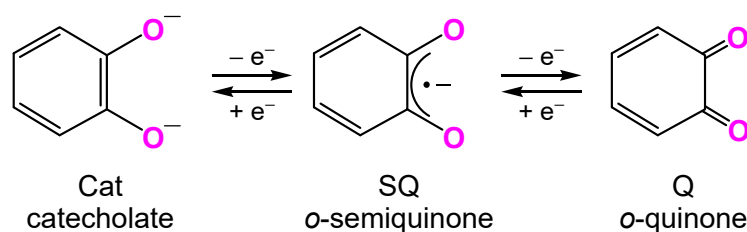

Scheme 1. Redox isomers of catechol.

We report herein our catecholato copper(II) chemistry with sterically hindered neutral tris(3,5-diisopropyl-1-pyrazolyl)methane (L1') and anionic hydrotris(3,5-diisopropyl-1-pyrazolyl)borate (L1$^-$), as shown in Scheme 2. The structures of catecholato and *o*-semiquinonato copper(II) complexes have been determined and deposited in the Cambridge Structural Database [25]. Their structural parameters are listed in Scheme 3 and Table 1 [26–37]. The reported catechol-copper(II) coordination can be divided into two groups: catecholato copper(II) complex and *o*-semiquinonato copper(II) complex. Regarding the structural parameters of catechol-copper(II) coordination, it can be characterized by the bond lengths of *d* (C–O) and *d* (C1–C2) in catechol: > 1.3 Å and < ~1.45 Å for catecholato copper(II) complex and < 1.3 Å and > ~1.45 Å for *o*-semiquinonato copper(II) complex, respectively. The magnetic properties in catechol-copper(II) coordination may also provide good evidence for defining the redox isomers of catechol. With the foregoing in mind and motivated to obtain greater insight into the structural and spectroscopic differences between hindered neutral L1' and anionic L1$^-$, we prepared three catecholato copper(II) complexes, namely **[Cu(catCl$_4$)(L1')]**, **[Cu(catBr$_4$)(L1')]**, and **[Cu(catCl$_4$)(L1H)]**. All complexes were characterized by single crystal X-ray crystallography and spectroscopic techniques, viz. IR/far-IR, UV-Vis, and ESR spectroscopy. Several decisive differences in their structures and physicochemical properties of catecholato copper(II) complexes were observed and are discussed in detail.
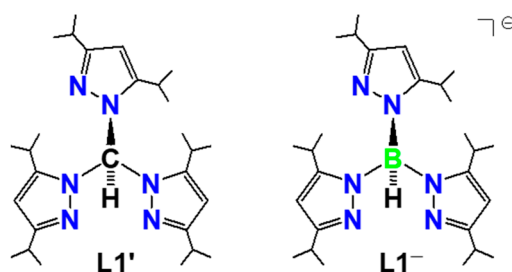
Scheme 2. Ligands in this research.
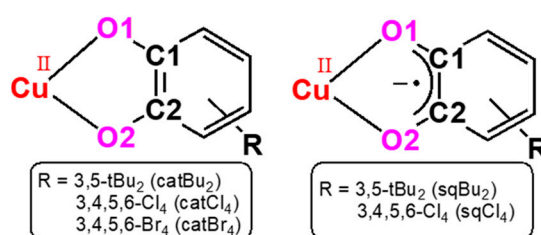
Scheme 3. Schematic drawing of two types of copper(II) complexes in Table 1.

Table 1. Structural parameters of selected catecholato and *o*-semiquinonato copper(II) complexes.

Complex	d (Cu–O) / Å	d (C–O) / Å	d (C1–C2) / Å	Reference
catecholato complex				
[Cu(catCl₄)(L1′)]	1.9280(14) 1.9106(18)	1.316(3) 1.318(2)	1.425(3)	this work
[Cu(catBr₄)(L1′)]	1.929(2) 1.905(3)	1.318(5) 1.318(4)	1.421(5)	this work
[Cu(catCl₄)(L1H)]	1.890(4) 1.952(4)	1.336(8) 1.334(6)	1.412(8)	this work
[Cu(catBu₂)(bipy)(MeOH)] [a]	1.929(2) 1.898(2)	1.344(4) 1.342(4)	1.422(4)	[26]
[Cu(catBu₂)(DBED)] [a]	1.943(2) 1.924(2)	1.347(3) 1.349(3)	1.425(4)	[27]
[Cu(catBu₂)(Me₃-tacn)] [a,b]	1.911(3) 1.903(3)	1.343(5) 1.346(4)	1.421(5)	[28]
	1.932(2) 1.895(3)	1.341(5) 1.353(4)	1.420(5)	
[Cu(catBu₂)(py)₂](BF₄) [b]	1.964(2) 1.919(2)	1.354(4) 1.335(4)	1.423(6)	[29]
	1.964(2) 1.908(2)	1.367(3) 1.336(4)	1.408(4)	
[Cu(catBu₂)(bpy)]	1.901(5) 1.870(5)	1.364(8) 1.338(8)	1.407(10)	[30]
[Cu(catCl₄)Cu(H₂O)₂(μ-py1)](ClO₄)₂ [a]	1.933(2) 1.934(2)	1.339(4) 1.344(4)	1.412(5)	[31]
[Cu(catCl₄)Cu(H₂O)(μ-py2)](ClO₄)₂ [a,b]	1.918(3) 1.979(3)	1.322(6) 1.337(6)	1.401(7)	[31]
	1.939(3) 1.984(3)	1.336(6) 1.333(5)	1.407(7)	
[Cu(catCl₄)Cu(H₂O)(μ-py3)](ClO₄)₂ [a]	1.9684(17). 1.9465(17)	1.333(3) 1.328(3)	1.421(3)	[31]
[Cu(catCl₄)(bispidine1)] [a]	2.456(2) 1.909(2)	1.301(3) 1.313(3)	1.440(3)	[32]
[{Cu(catCl₄)}₂(μ-bispidine2)] [a,b]	1.947(4) 1.899(4)	1.340(7) 1.336(7)	1.416(9)	[32]
	1.914(3) 1.930(5)	1.316(8) 1.324(6)	1.429(9)	
[Cu(catCl₄)(Bn₃-tacn)] [a]	1.940(4) 1.915(4)	1.335(7) 1.317(6)	1.430(7)	[33]

Table 1. *Cont.*

Complex	d (Cu–O) / Å	d (C–O) / Å	d (C1–C2) / Å	Reference
o-semiquinonato complex				
[Cu(sqBu$_2$)(DPyA)(thf)$_2$](BF$_4$) [a]	1.977(3) 1.978(2)	1.297(4) 1.276(5)	1.461(5)	[26]
[Cu(sqBu$_2$)(bipy)](BF$_4$) [a]	1.933(3) 1.936(3)	1.293(6) 1.287(5)	1.452(7)	[26]
[Cu(sqBu$_2$)(DBED)](SbF$_6$) [a]	1.975(2) 1.924(2)	1.285(3) 1.269(3)	1.464(4)	[27]
[Cu(sqBu$_2$)(TMCD)](SbF$_6$) [a]	1.963(2) 1.949(2)	1.289(3) 1.291(3)	1.455(4)	[27]
[Cu(sqCl$_4$)(Bn$_3$-tacn)] [a]	1.988(5) 2.001(4)	1.272(6) 1.265(7)	1.435(8)	[33]
[Cu(sqBu$_2$)(EtO)]$_2$ [b]	1.952(4) 1.949(5)	1.261(7) 1.294(7)	1.477(9)	[34]
	1.934(5) 1.945(5)	1.309(8) 1.275(9)	1.444(9)	
[Cu(sqBu$_2$)(Tp^{Cum,Me})] [a]	1.952(3) 1.971(3)	1.279(5) 1.265(6)	1.457(7)	[35]
[Cu(sqBu$_2$)$_2$]$_2$ [b]	1.918(4) 1.955(4)	1.291(7) 1.296(6)	1.470(8)	[36]
	1.944(4) 1.941(4)	1.290(7) 1.296(6)	1.45(1)	
[Cu(sqBu$_2$){NH(Py)$_2$}](ClO$_4$)$_2$ [a,b]	1.962(5) 1.964(4)	1.293(7) 1.304(7)	1.446(9)	[37]
	1.934(5) 1.969(4)	1.289(7) 1.284(4)	1.45(1)	

[a] bipy = 2,2′-bipyridine, DBED = *N*,*N*′-di-*tert*-butylethane-1,2-diamine, Me$_3$-tacn = 1,4,7-trimethyl-1,4,7-triazacyclononane), py1 = μ$_2$-3,5-bis{*N*,*N*-dimethylaminoethyl(methyl)aminomethyl}pyrazolate, py2 = μ$_2$-3,5-bis{bis(2-(diethylamino)ethyl)aminomethyl}pyrazolate, py3 = μ$_2$-3,5-bis{*N*,*N*-dimethylaminoethyl(methyl) aminomethyl}pyrazolate, bispidine1 = 9,9-dihydroxy-1,5-bis(methoxycarbonyl)-3,7-dimethyl-2,4-bis(2-pyridyl)-3,7-diazabicyclo(3.3.1)nonane, bispidine2 = 7,7′-propano-bis(3-methyl-1,5-bis(methoxycarbonyl)-2,4-bis(2-pyridyl)-3,7-diazabicyclo(3.3.1)nonan-9-one, Bn$_3$-tacn = 1,4,7-tribenzyl-1,4,7-triazacyclononane, DPyA = *N*-(pyridin-2-yl) pyridin-2-amine, TMCD = *N*,*N*,*N*′,*N*′-tetramethylcyclohexane-1,2-diamine, Tp^{Cum,Me} = hydrotris(3-cumenyl -5-methylpyrazol-1-yl)borate, NH(Py)$_2$ = di-2-pyridylamine, [b] two crystallographically independent molecules.

2. Results and Discussion

2.1. Synthesis

All of the four complexes prepared as shown in Scheme 4 gave a satisfactory elemental analysis. The reaction of mononuclear chlorido copper(II) [CuCl$_2$(L1′)] with suitable catechols, catH$_2$X$_4$ (X = Cl and Br) and NEt$_3$ at −50 °C yielded green colored mononuclear catecholato complexes, **[Cu(CatCl$_4$)(L1′)]** and **[Cu(CatBr$_4$)(L1′)]**, respectively. On the other hand, purple colored mononuclear catecholato complex **[Cu(CatCl$_4$)(L1H)]** was synthesized using the binuclear hydroxido complex [{Cu(L1)}(μ-OH)]$_2$.
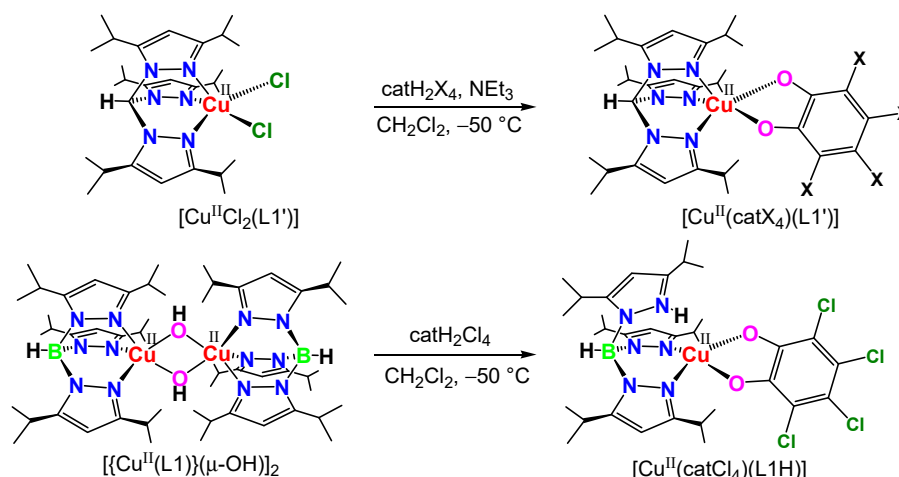
Scheme 4. Schematic drawing of the synthetic schemes of complexes.

2.2. Structure

Successful single-crystal X-ray structural analyses were performed on compounds **[Cu(catCl₄)(L1′)]**, **[Cu(catBr₄)(L1′)]**, and **[Cu(catCl₄)(L1H)]**. The perspective drawings of all three complexes are shown in Figures 1 and 2. The selected bond distances and bond angles of the obtained complexes are summarized in their figure captions.
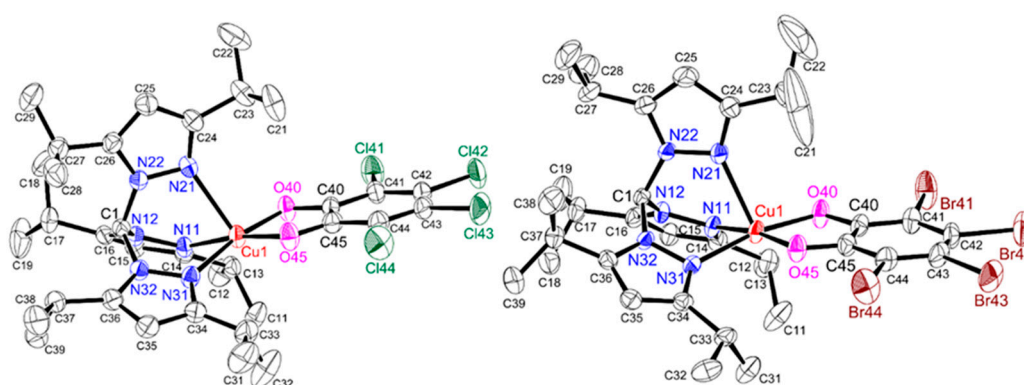
Figure 1. Crystal structures of **[Cu(catCl₄)(L1′)]** (**left**) and **[Cu(catBr₄)(L1′)]** (**right**) showing 50% displacement ellipsoids and the atom labeling scheme. Hydrogen atoms and solvents were omitted for reasons of clarity. Relevant bond lengths (Å) and angles (°): Cu1–N11, 2.036(2); Cu1–N21, 2.313(2); Cu1–N31, 2.044(2); Cu1–O40, 1.928(1); Cu1–O45, 1.911(2); C40–O40, 1.316(3); C45–O45, 1.318(2); C40–C45, 1.425(3); N11–Cu1–N21, 83.90(7); N11–Cu1–N31, 86.95(7); N21–Cu1–N31, 86.54(7); N11–Cu1–O40, 94.10(6); N21–Cu1–O40, 102.93(6); N31–Cu1–O40, 170.53(8); N11–Cu1–O45, 171.90(7); N21–Cu1–O45, 103.86(7); N31–Cu1–O45, 91.16(7); O40–Cu1–O45, 86.49(7). Cu1–N11, 2.023(3); Cu1–N21, 2.304(3); Cu1–N31, 2.053(2); Cu1–O40, 1.929(2); Cu1–O45, 1.905(3); C40–O40, 1.318(5); C45–O45, 1.318(4); C40–C45, 1.421(5); N11–Cu1–N21, 85.30(11); N11–Cu1–N31, 86.38(11); N21–Cu1–N31, 85.99(10); N11–Cu1–O40, 95.07(11); N21–Cu1–O40, 104.73(10); N31–Cu1–O40, 169.25(11); N11–Cu1–O45, 170.76(11); N21–Cu1–O45, 103.25(12); N31–Cu1–O45, 90.69(10); O40–Cu1–O45, 86.22(11).
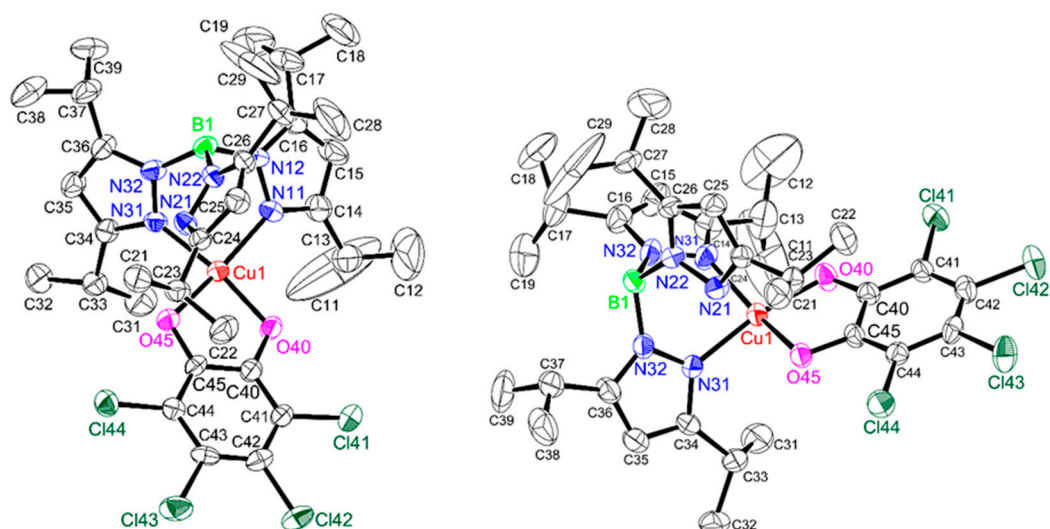
Figure 2. Crystal structure of **[Cu(catCl₄)(L1H)]** showing 50% displacement ellipsoids and the atom labeling scheme (**left**: top view, **right**: side view). Hydrogen atoms were omitted for reasons of clarity. Relevant bond lengths (Å) and angles (°): Cu1–N11, 1.976(5); Cu1–N31, 1.973(5); Cu1–O40, 1.890(4); Cu1–O45, 1.952(4); C40–O40, 1.336(8); C45–O45, 1.334(6); C40–C45, 1.412(8); N11–Cu1–N31, 91.2(2); N11–Cu1–O40, 96.1(2); N31–Cu1–O40, 169.3(2); N11–Cu1–O45, 159.1(2); N31–Cu1–O45, 89.36(19); O40–Cu1–O45, 86.61(17).

The coordination geometry around the copper(II) ion in **[Cu(catCl₄)(L1′)]** and **[Cu(catBr₄)(L1′)]** is essentially a five-coordinate square-pyramidal geometry with the basal plane comprising two nitrogen atoms (N11 and N31) from tris(pyrazolyl)methane and two oxygen atoms (O40 and O45) from catechol and whose axial site is occupied by the remaining nitrogen atom (N21) (Figure 1). This coordination geometry is supported by the structural parameter τ_5 values (0.02 in **[Cu(catCl₄)(L1′)]** and 0.03 in **[Cu(catBr₄)(L1′)]**) [38]. The apical deviation of the copper(II) ion from the corresponding least-squares N₂O₂ basal plane is 0.15 Å in **[Cu(catCl₄)(L1′)]** and 0.17 Å in **[Cu(catBr₄)(L1′)]**. The averaged Cu–O distances of 1.919(2) Å in **[Cu(catCl₄)(L1′)]** and 1.917(3) Å in **[Cu(catBr₄)(L1′)]** and the averaged C–O distances of 1.317(3) Å in **[Cu(catCl₄)(L1′)]** and 1.318(4) Å in **[Cu(catBr₄)(L1′)]**. In general, the C–O bond distances in catCl₄²⁻ (3,4,5,6-tetrachlorocatecholate) and sqCl₄•⁻ (3,4,5,6-tetrachloro-*o*-semiquinate) fall into the range of 1.30–1.36 Å and 1.26–1.31 Å, respectively (Table 1). Therefore, the coordinated catechol group in **[Cu(catCl₄)(L1′)]** and **[Cu(catBr₄)(L1′)]** is best described as catX₄²⁻, rather than either sqX₄•⁻ or qX₄ ((3,4,5,6-tetrahalogeno-*o*-quinone) (Scheme 1), and both copper are divalent. This oxidation assignment is consistent with the data of d-d transitions in UV-Vis spectra and ESR parameters in ESR spectra (vide infra). The dihedral angle between apical pyrazole and catechol ring is 99.3° in **[Cu(catCl₄)(L1′)]** and 90.0° in **[Cu(catBr₄)(L1′)]**. Therefore, the apical pyrazole locates in a nearly vertical position.

In contrast to the L1′ complexes, the L1⁻ complex is something different. Its structure revealed that hydrotris(pyrazolyl)borate adopts an unusual bidentate mode of coordination mode with one dangling pyrazole ring. The apical nitrogen (N21) is located away from the copper(II) center; the distance between Cu1 and N21 is 2.991(6) Å. The apical deviation of the copper(II) ion from the corresponding least-squares N₂O₂ basal plane is 0.11 Å, indicating that the coordination geometry around the copper(II) ion in **[Cu(catCl₄)(L1H)]** is essentially a four-coordinate square-planar geometry whose basal plane consists of two nitrogen atoms (N11 and N31) from hydrotris(pyrazolyl)borate and two oxygen atoms (O40 and O45) from catechol. The dihedral angle between apical pyrazole and catechol ring is 71.2°. The distance of N21···O40 is 4.112(7) Å and that of N21···O45 is 2.903(7) Å. Therefore, the dangling pyrazole ring is tilted toward N31 pyrazole ring. From the averaged Cu–O distances of 1.921(4) Å and the averaged C–O distances of 1.335(8) Å, the coordinated catechol group is best described as catCl₄²⁻ rather than either sqCl₄•⁻ or qCl₄ (Scheme 1 and Table 1) as well as the L1′ complexes and

this copper is also divalent. This oxidation assignment is also consistent with the UV-Vis and ESR data (vide infra). The charge consideration of the catechol and the copper oxidation state indicates the anionic hydrotris(pyrazolyl)borate should be neutral. This unusual behavior suggests the dangling pyrazole must be protonated at the apical nitrogen (N21). This behavior is supported by ν(N–H) in its IR spectrum (vide infra) and intramolecular hydrogen bond between N21 and O45 (2.903(7) Å). This protonated hydrotris(pyrazolyl)borate is very rare. The first example of copper(II) complex was reported by Professor S. Trofimenko in 1994 [39]. Other reported examples include V(IV) complex [40], Mn(II) complex [41], Pt(II) complexes [42–44], and Pt(IV) complex [45].
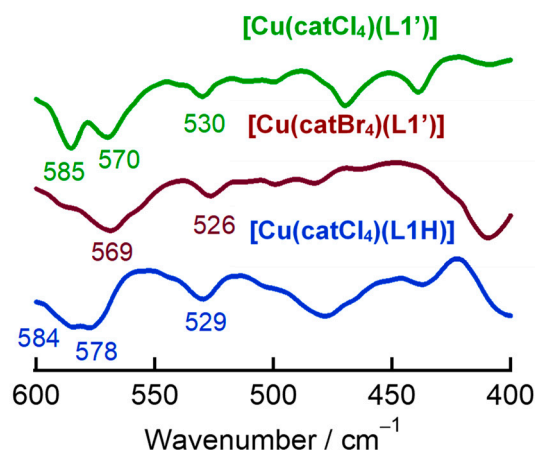
2.3. IR Spectroscopy

IR spectra of the three catecholato complexes were measured using KBr pellets as shown in Figure 3. One typical C=N stretching vibration in both **[Cu(catCl₄)(L1')]** and **[Cu(catBr₄)(L1')]** complexes was shifted to 1557 and 1556 cm^{-1} from the corresponding L1' ligand at 1553 cm^{-1}, respectively [9]. Coordinated catechols typically show two strong stretching bands attributed to the ring stretching (ν(C–C)) and the CO group stretching (ν(C–O)) around ~1500 cm^{-1} and ~1350 cm^{-1}, respectively [46–50]. In the L1' complexes **[Cu(catCl₄)(L1')]** and **[Cu(catBr₄)(L1')]**, two broad characteristic bands were observed at 1466 and 1400 cm^{-1}, corresponding to the ring stretching (ν(C–C)) and the CO group stretching (ν(C–O)), respectively. In the L1$^-$ complex **[Cu(catCl₄)(L1H)]**, the ν(C=N) band split to 1569 and 1537 cm^{-1} due to different pyrazole ring environment. Intensity and stretching energy indicate that former is derived from the protonated pyrazole ring. Catechol ring stretching was also observed at 1453 and 1377 cm^{-1}. Moreover, the ν(N–H) band was observed at 3142 cm^{-1}. This is the first observation of the protonated pyrazole by IR spectroscopy.
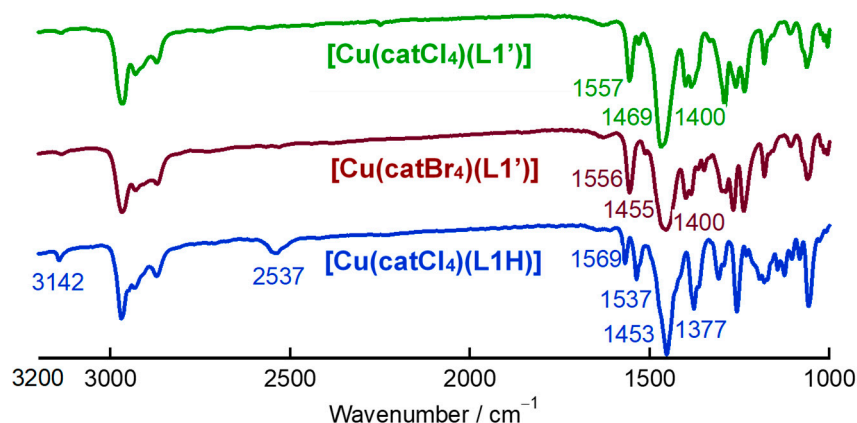
Figure 3. IR spectra of **[Cu(catCl₄)(L1')]** (**top**), **[Cu(catBr₄)(L1')]** (**middle**), and **[Cu(catCl₄)(L1H)]** (**bottom**) measured by KBr pellets.

Far-IR spectra of the three catecholato complexes were measured using CsI pellets as shown in Figure 4. From the literature, the M–O stretching bands of the coordinated catechol with transition metals were observed between 500 and 600 cm^{-1} [48–50]. However, the M–O stretching band values for the three catecholato complexes shown in Figure 4 are so broad and complicated that these assignments are very difficult at this stage and require more experiments and DFT calculations to make reliable assignments.

Figure 4. Far-IR spectra of **[Cu(catCl$_4$)(L1′)]** (**top**), **[Cu(catBr$_4$)(L1′)]** (**middle**), and **[Cu(catCl$_4$)(L1H)]** (**bottom**) measured by CsI pellets.

2.4. UV-Vis Spectroscopy

UV-Vis absorption spectra of the catecholato complexes **[Cu(catCl$_4$)(L1′)]**, **[Cu(catBr$_4$)(L1′)]**, and **[Cu(catCl$_4$)(L1H)]** are shown in Figure 5. As mentioned in Section 2.1, the structures of the L1′ complexes **[Cu(catCl$_4$)(L1′)]** and **[Cu(catBr$_4$)(L1′)]** contain a five-coordinate square-pyramidal geometry. This indicates that the d-d transition energies of the L1′ complexes are almost identical at 659 and 971 nm for **[Cu(catCl$_4$)(L1′)]** and 654 and 972 nm for **[Cu(catBr$_4$)(L1′)]**. However, in **[Cu(catCl$_4$)(L1H)]**, a different energy was observed for its d–d transition at 830 nm. This energy gap is consistent with other copper(II) coordination chemistry [14,51–53]. In the visible region, the L1′ complexes **[Cu(catCl$_4$)(L1′)]** and **[Cu(catBr$_4$)(L1′)]** exhibit characteristic bands at 505 nm and 503 nm. This band attributes to catecholate^{2-} to Cu(II) CT transition. For the latter, an additional peak also appears at 380 nm. One the other hand, the L1$^-$ complex **[Cu(catCl$_4$)(L1H)]** has a moderately intense band at 494 nm. The differences in these CT bands indicate the colors of the complexes are different: L1′ complexes **[Cu(catCl$_4$)(L1′)]** and **[Cu(catBr$_4$)(L1′)]** are green and L1$^-$ complex **[Cu(catCl$_4$)(L1H)]** is purple.
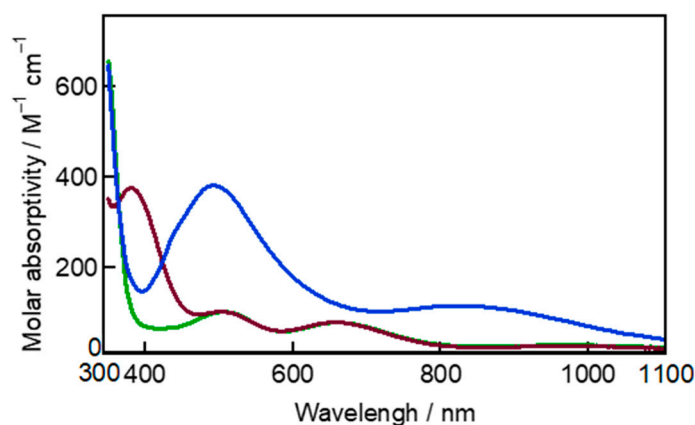
Figure 5. UV-Vis spectra of **[Cu(catCl$_4$)(L1′)]** (green), **[Cu(catBr$_4$)(L1′)]** (brown), and **[Cu(catCl$_4$)(L1H)]** (blue) measured by CH$_2$Cl$_2$ solution at 0 °C.

2.5. ESR Spectroscopy

The frozen glass ESR spectra of the complexes at 137 K are presented in Figure 6. The ESR spectra show that these complexes have an $S = 1/2$ ground state. The order of $g\| > g\perp > 2.0023$ is satisfied in all the complexes, confirming the presence of unpaired electron of the copper(II) ion in $d_{x^2-y^2}$ orbital. These observations are consistent with the above consideration that catechol is coordinated

as catecholate two minus anion. Some differences in the ESR parameters in all the complexes are caused by different coordination geometries: five-coordinate square-pyramidal and four-coordinate square-planar. The ESR parameters of the reported Cu(II)-catBu$_2$ or Cu(II)-catCl$_4$ complexes are also consistent with an $S = 1/2$ ground state [27–30,33]. On the other hand, the reported magnetism of Cu(II)-sqBu$_2$ or sqCl$_4$ complexes are diamagnetism (ESR silent) [27,33,34,36,37] or ferromagnetism [35].

[Cu(catCl$_4$)(L1')]

[Cu(catBr$_4$)(L1')]

[Cu(catCl$_4$)(L1H)]

2500   3000   3500

Magnetic field / gauss
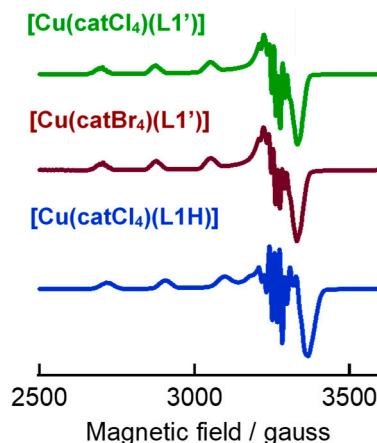
Figure 6. ESR spectra of **[Cu(catCl$_4$)(L1')]** (**top**), **[Cu(catBr$_4$)(L1')]** (**middle**), and **[Cu(catCl$_4$)(L1H)]** (**bottom**) measured by CH$_2$Cl$_2$/C$_2$H$_4$Cl$_2$ solution at 137 K.

3. Materials and Methods

3.1. Material and General Techniques

Preparation and handling of all the complexes was performed under an argon atmosphere using standard Schlenk tube techniques or in a VAC inert atmosphere glovebox containing argon gas. Dichloromethane and acetonitrile were carefully purified by refluxing and distilling under an argon atmosphere over phosphorous pentoxide and calcium hydride prior to use, respectively [54]. Other reagents are commercially available and were used without further purification. [CuCl$_2$(L1')] [8,11] and [{Cu(L1)}(μ-OH)]$_2$ [55] were prepared using the published methods.

3.2. Instrumentation

IR spectra (4000–400 cm^{-1}) and far-IR (650–150 cm^{-1}) spectra were recorded on KBr pellets and on CsI pellets, respectively, using a JASCO FT/IR-550 spectrophotometer (JASCO, Tokyo, Japan). Abbreviations used in the description of the vibration data are as follows: vs, very strong; s, strong; m, medium; w, weak. UV-Vis spectra at low temperature were measured on an Otsuka Electronics MCPD-2000 system (Otsuka Electronics, Tokyo, Japan) with an optical fiber attachment (300–1100 nm). ESR spectra as frozen solutions (dichloromethane/1,2-dichloroethane) were recorded on a Bruker EMX-T ESR spectrometer (Bruker Japan, Yokohama, Japan) at 137 K in quartz tubes (diameter 5 mm) with a liquid nitrogen temperature controller BVT 3000. The elemental analyses (C, H, N) were performed by the Chemical Analysis Center at the University of Tsukuba.

3.3. Preparation of Complexes

3.3.1. **[Cu(catCl$_4$)(L1')]**

To a solution of [CuCl$_2$(L1')] (160 mg, 0.266 mmol) in dichloromethane (40 cm^3) was added tetrachlorocatechol (81.5 mg, 0.329 mmol) and triethylamine (72.6 mg, 0.717 mmol) dissolved in dichloromethane (10 cm^3) at −50 °C and the solution was stirred at −50 °C for 30 min. During the reaction, the color of the solution gradually turned from yellow-green to green. After it was stirred at 0 °C for 30 min, the solvent was evaporated under vacuum. The resulting solid was extracted

with acetonitrile (40 mL). The filtrate was evaporated under vacuum and green powder was obtained. The green crystals were crystallized from acetonitrile at −30 °C. Single crystals were obtained from acetonitrile at −30 °C.

Yield: 75% (155 mg, 0.200 mmol). Calcd for $C_{34}H_{46}Cl_4CuN_6O_2$: C, 52.62; H, 5.97; N, 10.83. Found: C, 52.48; H, 6.19; N, 10.81. IR (KBr, ν/cm^{-1}): 2966 s, 2930 m, 2871 m, 1557 m, 1469 vs, 1400 m, 1385 m, 1292 s, 1237 m, 1181 m, 1110 w, 1064 m, 975 s, 803 s, 725 w, 669 m. Far-IR (CsI, ν/cm^{-1}): 635 w, 585 vs, 570 vs, 530 m, 470 s, 439 m, 409 w, 366 m, 329 s, 282 vs, 237 w, 211 vs. EPR (137 K, dichloromethane/1,2-dichloroethane) $g\|$ 2.30, $A\|$ 161 G, $g\perp$ 2.07, $A\perp$ 15 G. 161 G. UV-Vis (dichloromethane, λ_{max}/nm (ε/cm^{-1} mol^{-1} dm^3)) at 273 K: 505 (100), 659 (80), 971 (30).

3.3.2. **[Cu(catBr₄)(L1′)]**

To a solution of [CuCl₂(L1′)] (108 mg, 0.180 mmol) in dichloromethane (25 cm³) was added tetrabromocatechol (87.0 mg, 0.204 mmol) and triethylamine (43.6 mg, 0.431 mmol) dissolved in dichloromethane (10 cm³) at −50 °C, and the solution was stirred at −50 °C for 30 min. The color of the solution gradually turned from yellow-green to green. After it was stirred at 0 °C for 30 min, the solvent was evaporated under vacuum. The resulting solid was extracted with acetonitrile (50 mL). The filtrate was evaporated under vacuum and green powder was obtained. The green crystals were crystallized from acetonitrile at −30 °C. Single crystals were obtained from acetonitrile at −30 °C.

Yield: 75% (129 mg, 0.135 mmol). Calcd for $C_{34}H_{46}Br_4CuN_6O_2$: C, 42.81; H, 4.86; N, 8.81. Found: C, 42.60; H, 4.70; N, 8.74. IR (KBr, ν/cm^{-1}): 2967 s, 1556 m, 1455 vs, 1400 m, 1268 s, 1238 s, 1181 w, 1062 m, 927 m, 823 s, 739 m, 669 w. Far-IR (CsI, ν/cm^{-1}): 637 w, 616 s, 569 s, 526 m, 499 w, 483 w, 410 vs, 358 s, 304 m, 255 vs, 202 s. EPR (137 K, dichloromethane/1,2-dichloroethane) $g\|$ 2.28, $A\|$ 163 G, $g\perp$ 2.06, $A\perp$ 15 G. UV-Vis (dichloromethane, λ_{max}/nm (ε/cm^{-1} mol^{-1} dm^3)) at 273 K: 380 (380), 503 (100), 659 (80), 985 (30).

3.3.3. **[Cu(catCl₄)(L1H)]**

To a solution of [{Cu(L1)}(μ-OH)]₂ (221 mg, 0.203 mmol) in dichloromethane (20 cm³) was added tetrachlorocatechol (116 mg, 0.468 mmol) dissolved in dichloromethane (15 cm³) at −50 °C, and the solution was stirred at −50 °C for 30 min. The color of the solution gradually turned purple. After it was stirred at 0 °C for 30 min, the solution was concentrated under vacuum. After this, the solution was cooled at −50 °C to give purple crystals. Single crystals were obtained from dichloromethane at −50 °C.

Yield: 59% (186 mg, 0.240 mmol). Anal. Calcd for $C_{33}H_{47}BCl_4CuN_6O_2$: C, 51.08; H, 6.11; N, 10.83. Found: C, 50.87; H, 6.03; N, 10.56. IR (KBr, ν/cm^{-1}): 3142 w, 2969 s, 2871 m, 2537 w, 1569 m, 1537 m, 1453 vs, 1377 s, 1308 m, 1258 s, 1181 m, 1059 s, 972 s, 805 s, 741 m, 634 w. Far-IR (KBr, ν/cm^{-1}): 640 s, 578 s, 529 m, 478 s, 438 w, 397 s, 329 m, 285 vs, 220 s, 175 w. EPR (137 K, dichloromethane/1,2-dichloroethane) $g\|$ 2.27, $A\|$ 156 G, $g\perp$ 2.06, $A\perp$ 16 G. UV-Vis (dichloromethane, λ_{max}/nm (ε/cm^{-1} mol^{-1} dm^3)) at 273 K: 494 (380), 830 (120); at 223 K: 490 (400), 821 (120); at 195 K: 488 (440), 821 (130).

3.4. X-Ray Crystal Structure Determination

Crystal data and refinement parameters for the three catecholato copper(II) complexes **[Cu(catCl₄)(L1′)]**·2.5(CH₃CN), **[Cu(catBr₄)(L1′)]**·2.5(CH₃CN), and **[Cu(catCl₄)(L1H)]** are given in Table 2. All crystallographic data have been deposited at the CCDC, 12 Union Road, Cambridge CB2 1EZ, UK and copies can be obtained on request, free of charge, by quoting the publication citation and the deposition numbers. CCDC numbers: 620467 for **[Cu(catCl₄)(L1′)]**·2.5(CH₃CN), 620468 for **[Cu(catBr₄)(L1′)]**·2.5(CH₃CN), and 620469 for **[Cu(catCl₄)(L1H)]** (CIF and the checkCIF output files can be found at Supplementary Materials).

Table 2. Crystal data and structure refinement of copper complexes.

Complex	[Cu(catCl$_4$)(L1′)]· 2.5(CH$_3$CN)	[Cu(catBr$_4$)(L1′)]· 2.5(CH$_3$CN)	[Cu(catCl$_4$)(L1H)]
CCDC number	620467	620468	620469
Empirical Formula	C$_{39}$H$_{53.5}$Cl$_4$CuN$_{8.5}$O$_2$	C$_{39}$H$_{53.5}$Br$_4$CuN$_{8.5}$O$_2$	C$_{33}$H$_{47}$BCl$_4$CuN$_6$O$_2$
Formula Weight	878.77	1056.57	775.94
Crystal System	Monoclinic	Monoclinic	Monoclinic
Space Group	*C*2/*c* (#15)	*C*2/*c* (#15)	*P*2/*c* (#13)
a/Å	19.7412(11)	19.834(7)	15.405(7)
b/Å	15.9152(8)	16.302(5)	13.137(6)
c/Å	29.637(2)	29.749(10)	21.004(10)
β/°	103.9780(9)	107.918(3)	101.852(6)
V/Å^3	9035.8(10)	9152(5)	4160(3)
Z	8	8	4
D_{calc}/g cm^{-3}	1.292	1.533	1.239
μ(MoKα)/cm^{-1}	7.616	40.222	8.160
Temperature/°C	−71	−69	−61
2θ Range/°	6–55	6–55	6–55
Reflections Collected	30283	35994	33408
Unique Reflections	10131	10344	9475
R_{int}	0.0366	0.0410	0.0710
Number of Variables	504	504	424
Reflections/Parameter Ratio	20.16	20.52	22.35
Residuals: R_1 ($I > 2\sigma(I)$)	0.0476	0.0581	0.1099
Residuals: R (All Reflections)	0.0519	0.0768	0.1477
Residuals: wR_2 (All Reflections)	0.1187	0.1118	0.2762
Goodness of Fit Indicator	1.139	1.145	1.110
Max/Min Peak/e Å^{-3}	0.32/−0.36	1.07/−0.68	1.05/−0.73

$R_1 = \Sigma \, ||Fo| - |Fc||/\Sigma \, |Fo|$, $wR_2 = [\Sigma \, (w(Fo^2 - Fc^2)^2)/\Sigma \, w(Fo^2)^2]^{1/2}$.

The diffraction data were measured on a Rigaku/MSC Mercury CCD system (Rigaku, Tokyo, Japan) with graphite monochromated Mo Kα (λ = 0.71070 Å) radiation at low temperature. The unit cell parameters of each crystal were determined using CrystalClear [56] from 6 images. The crystal to detector distance was ca. 45 mm. Data were collected using 0.5° intervals in φ and ω to a maximum 2θ value of 55.0°. A total of 744 oscillation images were collected. The highly redundant data sets were reduced using CrystalClear and corrected for Lorentz and polarization effects [56]. An empirical absorption correction was applied for each complex. Structures were solved by direct methods (SIR92 and SIR97) [57,58] and heavy-atom Patterson methods [59]. The position of the copper ions and their first coordination sphere were located from a direct method *E*-map; other non-hydrogen atoms were found in alternating difference Fourier syntheses, and least squares refinement cycles. During the final refinement cycles the temperature factors were refined anisotropically. Refinement was carried out by a full matrix least-squares method on F^2. All calculations were performed with the CrystalStructure [60] crystallographic software package except for refinement, which was performed using SHELXL 2013 [61]. Hydrogen atoms were placed in calculated positions. Sheldrick weighting scheme was used. Crystallographic data and structure refinement parameters including the final discrepancies (*R* and *Rw*) are listed in Table 2. The crystals of **[Cu(catCl$_4$)(L1H)]** show a slightly lower quality of diffraction and some carbon atoms were disordered. Moreover, the solvent molecules in this crystal were highly disordered. Therefore, PLATON SQUEEZE was used to account for severely disordered solvent molecules [62].

4. Conclusions

The three catecholato copper(II) complexes **[Cu(catCl₄)(L1′)]**, **[Cu(catBr₄)(L1′)]**, and **[Cu(catCl₄)(L1H)]** ligated by sterically hindered neutral tris(3,5-diisopropyl-1-pyrazolyl)methane (L1′) and anionic hydrotris(3,5-diisopropyl-1-pyrazolyl)borate (L1⁻) were synthesized and characterized. The structures of the synthesized complexes were as follows: the L1′ complexes, **[Cu(catCl₄)(L1′)]** and **[Cu(catBr₄)(L1′)]**, adopted a five-coordinate square-pyramidal geometry, whereas the L1⁻ complex **[Cu(catCl₄)(L1H)]** adopted a four-coordinate square-planar geometry. In **[Cu(catCl₄)(L1H)]**, a protonated pyrazole was found to be present in the apical position to neutralize its charge. This anomalous N–H bond was observed in its IR spectrum. To our knowledge, this is the first direct proof for this protonated nitrogen in hydrotris(pyrazolyl)borate. These geometrical changes in catecholato copper(II) complexes were their d–d and CT transitions in UV-Vis absorption spectra and ESR parameters in ESR spectra. The direct structural and physicochemical changes due to different ligand charges were observed. Therefore, several tris(pyrazolyl)methane ligands were extensively explored [63,64]. We are also underway in determining how the structure of transition metals is affected by ligand charges and environments. Moreover, the anti-oxidant activity of our redox catecholato copper(II) complexes is also of interest.

References

1. Trofimenko, S. Boron-pyrazole chemistry. *J. Am. Chem. Soc.* **1966**, *88*, 1842–1844. [CrossRef]

2. Trofimenko, S.; Calabrese, J.C.; Thompson, J.S. Novel polypyrazolylborate ligands: Coordination control through 3-substituents of the pyrazole ring. *Inorg. Chem.* **1987**, *26*, 1507–1514. [CrossRef]

3. Trofimenko, S. *Scorpionates: The Coordination Chemistry of Polypyrazolylborate Ligands*; Imperial College Press: London, UK, 1999.

4. Pettinari, C. *Scorpionates II: Chelating Borate Ligands*; Imperial College Press: London, UK, 2008.

5. Trofimenko, S. Geminal poly(1-pyrazolyl)alkanes and their coordination chemistry. *J. Am. Chem. Soc.* **1970**, *92*, 5118–5126. [CrossRef]

6. Juliá, S.; Del Mazo, J.M.; Avila, L.; Elguero, J. Improved synthesis of polyazolylmethanes under solid-liquid phase-transfer catalysis. *Org. Prep. Proced. Int.* **1984**, *16*, 299–307. [CrossRef]

7. Reger, D.L.; Grattan, T.C.; Brown, K.J.; Little, C.A.; Lamba, J.J.S.; Rheingold, A.L.; Sommer, R.D. Syntheses of tris(pyrazolyl)methane ligands and {[tris(pyrazolyl)methane]Mn(CO)₃}SO₃CF₃ complexes: Comparison of ligand donor properties. *J. Organomet. Chem.* **2000**, *607*, 120–128. [CrossRef]

8. Fujisawa, K.; Ono, T.; Aoki, H.; Ishikawa, Y.; Miyashita, Y.; Okamoto, K.; Nakazawa, H.; Higashimura, H. Copper(II) complexes with a novel tris(3,5-diisopropyl-1-pyrazolyl)methane ligand, [Cu(X₂){HC(3,5-ⁱPr₂pz)₃}] (X = Cl and NO₃). *Inorg. Chem. Commun.* **2004**, *7*, 330–332. [CrossRef]

9. Fujisawa, K.; Ono, T.; Ishikawa, Y.; Amir, N.; Miyashita, Y.; Okamoto, K.; Lehnert, N. Structural and electronic differences of copper(I) complexes with tris(pyrazolyl)methane and hydrotris(pyrazolyl)borate ligands. *Inorg. Chem.* **2006**, *45*, 1698–1713. [CrossRef]

10. Fujisawa, K.; Iwamoto, H.; Tobita, K.; Miyashita, Y.; Okamoto, K. Copper(II) nitrato and chloro complexes with sterically hindered tridentate ligands: Influence of ligand framework and charge on their structure and physicochemical properties. *Inorg. Chim. Acta* **2009**, *362*, 4500–4509. [CrossRef]

11. Fujisawa, K.; Tobita, K.; Sakuma, S.; Savard, D.; Leznoff, D.B. Binuclear and mononuclear copper(II) chlorido complexes with hindered neutral N3 type ligands: Influence of ligand framework and charge on their structure and physicochemical properties. *Inorg. Chim. Acta* **2019**, *486*, 582–588. [CrossRef]

12. Lehnert, N.; Cornelissen, U.; Neese, F.; Ono, T.; Noguchi, Y.; Okamoto, K.; Fujisawa, K. Synthesis and spectroscopic characterization of copper(II)–nitrito complexes with hydrotris(pyrazolyl)borate and related coligands. *Inorg. Chem.* **2007**, *46*, 3916–3933. [CrossRef]

13. Quist, D.A.; Diaz, D.E.; Liu, J.L.; Karlin, K.D. Activation of dioxygen by copper metalloproteins and insights from model complexes. *J. Biol. Inorg. Chem.* **2017**, *22*, 253–288. [CrossRef] [PubMed]

14. Solomon, E.I.; Heppner, D.E.; Johnston, E.M.; Ginsbach, J.W.; Cirera, J.; Qayyum, M.; Kieber-Emmons, M.T.; Kjaergaard, C.H.; Hadt, R.G.; Tian, L. Copper active sites in biology. *Chem. Rev.* **2014**, *114*, 3659–3853. [CrossRef] [PubMed]

15. Qayyum, M.F.; Sarangi, R.; Fujisawa, K.; Stack, T.D.P.; Karlin, K.D.; Hodgson, K.O.; Hedman, B.; Solomon, E.I. L-Edge X-ray absorption spectroscopy and DFT calculations on Cu_2O_2 species: Direct electrophilic aromatic attack by side-on peroxo bridged dicopper(II) complexes. *J. Am. Chem. Soc.* **2013**, *135*, 17417–17431. [CrossRef] [PubMed]

16. Mirica, L.M.; Vance, M.; Rudd, D.J.; Hedman, B.; Hodgson, K.O.; Solomon, E.I.; Stack, T.D.P. Tyrosinase reactivity in a model complex: An alternative hydroxylation mechanism. *Science* **2005**, *308*, 1890–1892. [CrossRef]

17. Tezgerevska, T.; Alley, K.G.; Boskovic, C. Valence tautomerism in metal complexes: Stimulated and reversible intramolecular electron transfer between metal centers and organic ligands. *Coord. Chem. Rev.* **2014**, *268*, 23–40. [CrossRef]

18. Luca, O.R.; Crabtree, R.H. Redox-active ligands in catalysis. *Chem. Soc. Rev.* **2013**, *42*, 1440–1459. [CrossRef]

19. Kaim, W.; Schwederski, B. Non-innocent ligands in bioinorganic chemistry—An overview. *Coord. Chem. Rev.* **2010**, *254*, 1580–1588. [CrossRef]

20. Ray, K.; Petrenko, T.; Wieghardt, K.; Neese, F. Joint spectroscopic and theoretical investigations of transition metal complexes involving non-innocent ligands. *Dalton Trans.* **2007**, 1552–1566. [CrossRef]

21. Zanello, P.; Corsini, M. Homoleptic, mononuclear transition metal complexes of 1,2-dioxolenes: Updating their electrochemical-to-structural (X-ray) properties. *Coord. Chem. Rev.* **2006**, *250*, 2000–2022. [CrossRef]

22. Ward, M.D.; McCleverty, J.A. Non-innocent behaviour in mononuclear and polynuclear complexes: Consequences for redox and electronic spectroscopic properties. *Dalton Trans.* **2002**, 275–288. [CrossRef]

23. Pierpont, C.G. Unique properties of transition metal quinone complexes of the MQ_3 series. *Coord. Chem. Rev.* **2001**, *219–221*, 415–433. [CrossRef]

24. Pierpont, C.G. Studies on charge distribution and valence tautomerism in transition metal complexes of catecholate and semiquinonate ligands. *Coord. Chem. Rev.* **2001**, *216–217*, 99–125. [CrossRef]

25. Groom, C.R.; Bruno, I.J.; Lightfoot, M.P.; Ward, S.C. The Cambridge structural database. *Acta Cryst.* **2016**, *B72*, 171–179. [CrossRef] [PubMed]

26. Davidson, R.A.; Hao, J.; Rheingold, A.L.; Miller, J.S. High spin ground state copper(II) and nickel(II) complexes possessing the 3,5-di-*tert*-butyl-1,2-semiquinonate radical anion. *Polyhedron* **2017**, *133*, 348–357. [CrossRef]

27. Verma, P.; Weir, J.; Mirica, L.; Stack, T.D.P. Tale of a twist: Magnetic and optical switching in copper(II) semiquinone complexes. *Inorg. Chem.* **2011**, *50*, 9816–9825. [CrossRef]

28. Rall, J.; Wanner, M.; Albrecht, M.; Hornung, F.; Kaim, W. Sensitive valence tautomer equilibrium of paramagnetic complexes $[(L)Cu^{n+}(Q^{n-})]$ (n = 1 or 2; Q = quinones) related to amine oxidase enzymes. *Chem. Eur. J.* **1999**, *5*, 2802–2809. [CrossRef]

29. Speier, G.; Tisza, S.; Tyeklár, Z.; Lange, C.W.; Pierpont, C.G. Coligand-dependent shifts in charge distribution for copper complexes containing 3,5-di-*tert*-butylcatecholate and 3,5-di-*tert*-butylsemiquinonate ligands. *Inorg. Chem.* **1994**, *33*, 2041–2045. [CrossRef]

30. Buchanan, R.M.; Wilson-Blumenberg, C.; Trapp, C.; Larsen, S.K.; Greene, D.L.; Pierpont, C.G. Counterligand dependence of charge distribution in copper-quinone complexes. Structural and magnetic properties of (3,5-di-*tert*-butylcatecholato)(bipyridine)copper(II). *Inorg. Chem.* **1986**, *25*, 3070–3076. [CrossRef]

31. Ackermann, J.; Meyer, F.; Kaifer, E.; Pritzkow, H. Tuning the activity of catechol oxidase model complexes by geometric changes of the dicopper core. *Chem. Eur. J.* **2002**, *8*, 247–258. [CrossRef]
32. Börzel, H.; Comba, P.; Pritzkow, H. Structural studies on dicopper(II) compounds with catechol oxidase activity. *Chem. Commun.* **2001**, 97–98. [CrossRef]
33. Berreau, L.M.; Mahapatra, S.; Halfen, J.A.; Houser, R.P.; Young, V.G., Jr.; Tolman, W.B. Reactivity of peroxo- and bis(μ-oxo)dicopper complexes with catechols. *Angew. Chem. Int. Ed.* **1999**, *38*, 207–210. [CrossRef]
34. Bencini, A.; Dei, A.; Sangregorio, C.; Totti, F.; Vaz, M.G.F. Crystal and molecular structure and magnetic exchange properties of bis(di-μ-ethoxo-bis(3,5-di-*tert*-butylsemiquinonato)dicopper(II)) complex. A synergy between DFT and experimental magnetochemistry. *Inorg. Chem.* **2003**, *42*, 8065–8071. [CrossRef] [PubMed]
35. Ruf, M.; Noll, B.C.; Groner, M.D.; Yee, G.T.; Pierpont, C.G. Pocket semiquinonate complexes of cobalt(II), copper(II), and zinc(II) prepared with the hydrotris(cumenylmethylpyrazolyl)borate ligand. *Inorg. Chem.* **1997**, *36*, 4860–4865. [CrossRef] [PubMed]
36. Thompson, J.S.; Calabrese, J.C. Copper-catechol chemistry. Synthesis, spectroscopy, and structure of bis(3,5-di-*tert*-butyl-*o*-semiquinato)copper(II). *J. Am. Chem. Soc.* **1986**, *108*, 1903–1907. [CrossRef]
37. Thompson, J.S.; Calabrese, J.C. Synthesis, spectroscopy, and structures of copper(II)-3,5-di-*tert*-butyl-*o*-semiquinone complexes. *Inorg. Chem.* **1985**, *24*, 3167–3171. [CrossRef]
38. Addison, A.W.; Rao, T.N.; Reedijk, J.; van Rijn, J.; Verschoor, G.C. Synthesis, structure, and spectroscopic properties of copper(II) compounds containing nitrogen–sulphur donor ligands; the crystal and molecular structure of aqua[1,7-bis(*N*-methylbenzimidazol-2′-yl)-2,6-dithiaheptane]copper(II) perchlorate. *J. Chem. Soc. Dalton Trans.* **1984**, 1349–1356. [CrossRef]
39. Rheingold, A.L.; Haggerty, B.S.; Trofimenko, S. The first structurally characterized metal complex involving the free acid of a new tris(pyrazolyl)borate as ligand. *Angew. Chem. Int. Ed. Engl.* **1994**, *33*, 1983–1985. [CrossRef]
40. Kime-Hunt, E.; Spartalian, K.; DeRusha, M.; Nunn, C.M.; Carrano, C.J. Synthesis, characterization, and molecular structures of a series of [(3,5-dimethylpyrazolyl)borato]vanadium(III) and -(IV) complexes. *Inorg. Chem.* **1989**, *28*, 4392–4399. [CrossRef]
41. Singh, U.P.; Singh, R.; Hikichi, S.; Akita, M.; Moro-oka, Y. Characterization of a dinuclear Mn(II) tri(μ-carboxylato) complex with the hindered hydrotris(3,5-diisopropyl-1-pyrazolyl)borate (=Tp^{iPr2}) ligand: Intramolecular hydrogen bonding interaction between the protonated Tp^{iPr2} and Mn-coordinating carboxylate ligands. *Inorg. Chim. Acta* **2000**, *310*, 273–278.
42. Reinartz, S.; White, P.S.; Brookhart, M.; Templeton, J.L. Structural characterization of an intermediate in arene C–H bond activation and measurement of the barrier to C–H oxidative addition: A platinum(II) η^2-benzene adduct. *J. Am. Chem. Soc.* **2001**, *123*, 12724–12725. [CrossRef]
43. Norris, C.M.; Reinartz, S.; White, P.S.; Templeton, J.L. Barriers for arene C–H bond activation in platinum(II) η^2-arene intermediates. *Organometallics* **2002**, *21*, 5649–5656. [CrossRef]
44. Kostelansky, C.N.; MacDonald, M.G.; White, P.S.; Templeton, J.L. Stoichiometric alkane dehydrogenation with Tp′PtMe$_2$H to form Tp′Pt(η^2-olefin)(H) complexes. *Organometallics* **2006**, *25*, 2993–2998. [CrossRef]
45. Reinartz, S.; White, P.S.; Brookhart, M.; Templeton, J.L. Five-coordinate trispyrazolylborate dihydridosilyl platinum(IV) complexes. *J. Am. Chem. Soc.* **2001**, *123*, 6425–6426. [CrossRef] [PubMed]
46. Cuevas, A.; Geis, L.; Pintos, V.; Chiozzone, R.; Sanchíz, J.; Hummert, M.; Schumann, H.; Kremer, C. Synthesis, molecular structure and magnetic properties of a rhenium(IV) compound with catechol. *J. Mol. Struct.* **2009**, *921*, 80–84. [CrossRef]
47. Horsman, G.P.; Jirasek, A.; Vaillancourt, F.H.; Barbosa, C.J.; Jarzecki, A.A.; Xu, C.; Mekmouche, Y.; Spiro, T.G.; Lipscomb, J.D.; Blades, M.W.; et al. Spectroscopic studies of the anaerobic enzyme-substrate complex of catechol 1,2-dioxygenase. *J. Am. Chem. Soc.* **2005**, *127*, 16882–16891. [CrossRef]
48. Öhrström, L.; Michaud-Soret, I. Fe–catecholate and Fe–oxalate vibrations and isotopic substitution shifts from DFT quantum chemistry. *J. Phys. Chem. A* **1999**, *103*, 256–264. [CrossRef]
49. Edwards, C.F.; Griffith, W.P.; White, A.J.P.; Williams, D.J. New catecholato oxorhenium(V) complexes. *J. Chem. Soc. Dalton Trans.* **1992**, 957–962. [CrossRef]
50. Michaud-Soret, I.; Andersson, K.K.; Que, L., Jr. Resonance Raman studies of catecholate and phenolate complexes of recombinant human tyrosine hydroxylase. *Biochemistry* **1995**, *34*, 5504–5510. [CrossRef]
51. Solomon, E.I.; Szilagyi, R.K.; George, S.D.; Basumallick, L. Electronic structures of metal sites in proteins and models: Contributions to function in blue copper proteins. *Chem. Rev.* **2004**, *104*, 419–458. [CrossRef]

52. Hathaway, B.J. A new look at the stereochemistry and electronic properties of complexes of the copper(II) ion. *Struct. Bond.* **1984**, *57*, 55–118.

53. Hathaway, B.J.; Billing, D.E. The electronic properties and stereochemistry of mono-nuclear complexes of the copper(II) ion. *Coord. Chem. Rev.* **1970**, *5*, 143–207. [CrossRef]

54. Armarego, W.L.F.; Chai, C.L.L. *Purification of Laboratory Chemicals*, 7th ed.; Butterworth-Heinemann: Oxford, UK, 2013.

55. Kitajima, N.; Fujisawa, K.; Fujimoto, C.; Moro-oka, Y.; Hashimoto, S.; Kitagawa, T.; Toriumi, T.; Tatsumi, K.; Nakamura, A. A new model for dioxygen binding in hemocyanin. Synthesis, characterization, and molecular structure of the μ-η^2:η^2 peroxo dinuclear copper(II) complexes, $[Cu(HB(3,5-R_2pz)_3)]_2(O_2)$ (R = *i*-Pr and Ph). *J. Am. Chem. Soc.* **1992**, *114*, 1277–1291. [CrossRef]

56. *CrystalClear: Data Collection and Processing Software*; Rigaku Corporation: Tokyo, Japan, 2015.

57. Altomare, A.; Cascarano, G.; Giacovazzo, C.; Guagliardi, A. Completion and refinement of crystal structures with *SIR92*. *J. Appl. Cryst.* **1993**, *26*, 343–350. [CrossRef]

58. Altomare, A.; Burla, M.C.; Camalli, M.; Cascarano, G.L.; Giacovazzo, C.; Guagliardi, A.; Moliterni, A.G.G.; Polidori, G.; Spagna, R. *SIR97*: A new tool for crystal structure determination and refinement. *J. Appl. Cryst.* **1999**, *32*, 115–119. [CrossRef]

59. Beurskens, P.T.; Beurskens, G.; de Gelder, R.; García-Granda, S.; Israel, R.; Gould, R.O.; Smits, J.M.M. *The DIRDIF99 Program System, Technical Report of the Crystallography Laboratory*; University of Nijmegen: Nijmegen, The Netherlands, 1999.

60. *Crystal Structure 4.3: Crystal Structure Analysis Package*; Rigaku Corporation: Tokyo, Japan, 2018.

61. Sheldrick, G.M. *SHELXL Version 2014/3*: A short history of *SHELX*. *Acta Cryst.* **2008**, *A64*, 112–122. [CrossRef] [PubMed]

62. Spek, A.L. *PLATON SQUEEZE*: A tool for the calculation of the disordered solvent contribution to the calculated structure factors. *Acta Cryst.* **2015**, *71*, 9–18.

63. Martins, L.M.D.R.S.; Pombeiro, A.J.L. Tris(pyrazol-1-yl)methane metal complexes for catalytic mild oxidative functionalizations of alkanes, alkenes and ketones. *Coord. Chem. Rev.* **2014**, *265*, 74–88. [CrossRef]

64. Martins, L.M.D.R.S.; Pombeiro, A.J.L. Water-soluble C-scorpionate complexes—Catalytic and biological applications. *Eur. J. Inorg. Chem.* **2016**, *15–16*, 2236–2252. [CrossRef]